

A Radio Resource Management Scheme in future Ultra-Dense Phantom Networks

Antonio Di Maria, Daniela Panno

*Dept. Department of Electrical, Electronics and Computer Engineering, University of Catania, Italy
antoniodm@unict.it, daniela.panno@dieei.unict.it

Abstract—The Phantom cell concept is a solution for high-traffic outdoor environments that can also support good mobility and connectivity in ultra-dense network. In a phantom cells network, a centralized Macrocell controls all phantom cells within its coverage area and the C-Plane and U-Plane are split. Many issues need to be addressed for this architecture including radio resources allocation and cross/co tier interference mitigation. One of effective techniques used to mitigate interference is to group the cells in community (clusters). In this line, we propose a review of the max-min distance algorithm to establish the optimal cluster number, which affects significantly the system performance. Also, to assign the spectral resources to cells of the cluster, a new allocation algorithm based on traffic demand is proposed.

Keywords—ultra-dense networks; clustering; LTE; interference mitigation; spectral resource allocation

I. INTRODUCTION

The traffic volume in cellular networks has increased considerably during recent years and this trend is expected to continue at an exponential rate [1]. This is mostly due to the massive proliferation of intelligent mobile devices with ubiquitous and always-on connectivity and machine type communication which leads to the shifting of the dominant traffic type from mobile voice to mobile data and video.

Considering the statistics regarding the growth of traffic volume, in the near future even the existing 4G networks will be unable to satisfy the ever-increasing user requirements. To cope with the traffic growth expected for the following years, ultra-dense networks will be employed: the basic idea is to get the access nodes as close as possible to the end users. To satisfy Quality of Service (QoS) requirements over the region of interest, the next networks will be made up of multiple base stations which have different features, in terms of connected users (UEs), transmitted power and coverage areas (indoor small cell and outdoor macro and small cell deployments). In [6] is provided a quantitative measure of the cell density at which a network can be considered ultra-dense ($\geq 10^3$ cells/km²).

The Software Defined Networking (SDN) / Network Function Virtualization (NFV) paradigms are considered as the enabling technologies to realize these enhancements. In particular, (SDN) is responsible for decoupling control and data plane, whereas (NFV) permits to perform the abstraction of network functionalities from the underlying hardware [17]. In this context, the Phantom Cell Concept is proposed by DOCOMO in [3] as one solution for the next ultra-dense networks, based on Dual Connectivity scheme standardized

by 3GPP for Release 12 small cell enhancements [2]. In the Phantom cell solution, the base station of macrocell (eNodeB in LTE standard) controls all small cells, so called phantom cells, within its coverage area (macrocell). In addition, the control plane (C-Plane) and user data plane (U-Plane) are split, as shown in Fig. 1. For a UE in a phantom cell, the C-Plane is provided by the Macro eNodeB (M-eNB in the following) at low frequency band (2 GHz) to maintain good connectivity and mobility, while the U-Plane is provided by Phantom base station (Ph-eNB in the following), at higher frequency band (3.5 GHz) to boost user data rate. The Radio Resource Connection (RRC) procedures between UEs and Ph-eNBs (such as channel establishment and channel release) are managed by Macro eNodeB via the X3 interface (master-slave connection). As reported in [3], the backhaul link among Phantom and Macro cells can be relaxed, because they use different transmission points with independent baseband processing. So, optical fiber is not necessarily required. If a UE is only covered by M-eNB, this provides both C-Plane and U-Plane. The Ph-eNBs do not transmit cell-specific signals, such as primary synchronization signal (PSS), secondary synchronization signal (SSS). Instead, they transmit a new type of pilot symbols: Discovery Reference Signal (DRS) required for small cell discovery and initial channel estimation purposes [4]. More detailed information about DRS can be found in [5].

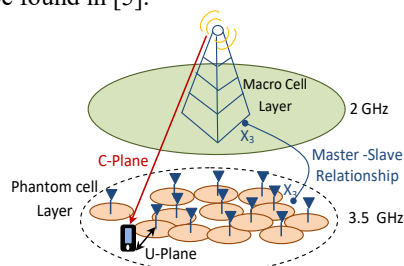


Fig. 1 Phantom cell Network Architecture

This new architecture has a range of benefits. First, the M-eNodeB plays a role of centralized decisional point by managing the small cell configuration. Second, the deployment of small cells on a dedicated carrier solves the cross-tier interference issue. Finally, in terms of scalability, it enables network operators to gradually add capacity increasing the number of cells. On the other hand, the densification of Phantom cells has a detrimental impact: the inter-cell interference in this layer becomes even more acute and intolerable. So, for a phantom network architecture, in order to maintain a high level of capacity, mitigate the co-tier interference is needed. At this aim, the basic idea is to allocate

disjoint portions of spectral resources to the Phantom cells which have critical interference relations trying to maximize the frequency reuse. However, an optimal solution to this purpose becomes harder when the number of cells increases. The above issue has already received a lot of attention, and several radio resource management schemes are available in literature. The proposed algorithms are based on different techniques, such as graph theory, game theory, or clustering methods [8-12].

Basing on clustering concept, we propose a two phases radio resource control scheme. In the first phase, the Ph-eNBs are grouped in two or more communities (clusters) by using a modified Max-Min Distance Algorithm (MMDA) and the key-means algorithm [7]. In the second phase, the whole bandwidth resource is dynamically subdivided between cells of each cluster, depending on actual users' traffic demand. In addition, in order to increase the capacity of the system, the whole bandwidth is reused in the remaining clusters by minimizing the co-cluster interference. For the first phase, we propose three variants of the MMDA: two solutions ensure static clustering operation once the topology of Ph-eNBs is fixed; the other adopts a dynamic clustering operation based on the UEs variable position. The last solution achieves best performance but increases the computational complexity.

We benchmark our approach to two schemes [10- 11] in literature. In [10], the authors propose a cluster-based two-stage resource management (CTRM) scheme for an indoor scenario where femtocells are used. Firstly, for the clustering procedure they use a modified key-means algorithm. Then, they propose a two-stage distributed sub-channel allocation scheme to maximize system throughput. In [11] a dynamic allocation scheme is proposed for ultra-dense outdoor scenarios. It is a centralized solution based on graph coloring technique to mitigate co-tier interference. This scheme (called Graph scheme in the following) takes into account the UE position and the traffic demand during allocation procedure.

The comparative analysis shows that our approach outperforms the considered reference schemes in terms of throughput in outdoor ultra-dense network.

The remainder of this paper is organized as follow. In Section II the system model is described. The proposed Clustering and Resource Allocation (CRA) scheme (in static and dynamic versions) is presented in Section III. Simulation results are showed in Section IV. Finally, the concluding remarks are given in Section V.

II. SYSTEM MODEL

We consider an urban area covered by a M-eNB. Inside the macro area, several Phantom cells and UEs are random distributed. Since the Phantom cell architecture assumes a C-plane/U-plane split configuration, where the C-plane is exclusively provided by macro base station (M-eNB), we introduce a centralized control unit embedded in the M-eNB. This unit has complete information about UEs and Ph-eNBs location. In addition, it manages the radio resources allocation in order to mitigate downlink co-tier interference. The downlink of a 3GPP LTE system is considered. The system bandwidth (B) is divided into Physical Resource Blocks (PRBs) of 180 kHz. Based on Signal to Interference plus Noise Ratio (SINR) in downlink, the control unit computes

the number of PRBs that each UE requires to satisfy its demand [15]. The coverage area of a Ph-eNB is determined by its Discovery Reference Signal Received Power (DRSRP) measured by UE which must be greater than a minimum value, $DRSRP_{min}$. The pool of Phantom cells may have partially overlapping coverage areas and the phantom cell selection is decided by the criterion of maximum DRSRP value received.

III. RADIO RESOURCE MANAGEMENT SCHEME

We propose a centralized RRM scheme based on cell clustering concept. The control scheme is designed for outdoor environments with several hotspots which have moderate-power base stations and a considerable number of connected UEs. Our Clustering and dynamical Resource Allocation (CRA) scheme consists of two phases described below.

A. First phase: Clustering procedure

This step associates the Ph-eNBs which have critical interference relations in a same cluster. The value of clusters number (K) is relevant factor. In fact, on the one hand a high K value maximizes the frequency reuse and consequently the system capacity, but on the other hand it significantly increases the interference between cells associated with different clusters.

Inspired by CTRM [10], firstly we determine the K value by using innovative versions of the Max-Min distance algorithm. Then, we employ the known key-means algorithm to select suitable Ph-eNBs for each cluster.

The Max-Min Distance Algorithm (MMDA) is employed to define a less arbitrary and more repeatable distribution of cluster groups based on data set P (set of Ph-eNBs coordinates in our case) and assuming at least two clusters are expected. In iterative way, a threshold T determines if a new cluster should be created. The final number of clusters " K " will be the input value for the k-means algorithm. The K value significantly affects the system performance and it is strongly influenced by used threshold T .

In the traditional MMDA [16], on basis of Euclidean norm concept, the threshold T is iteratively calculated as follow:

$$T = \frac{\sum_{i=1}^{N_c} \sum_{j=1}^{N_c} |z_i - z_j|}{\sum_{k=1}^{N_c-1} k(k+1)/2}, \quad (1)$$

where N_c is current centroids number and z_i is i -th centroid. Since the traditional MMDA has been implemented for image processing, it is unable to group Ph-eNBs based on critical interference relations between them and/or active users' positions. For this reason, we propose innovative variants of the Max-Min distance algorithm, where we prefix the T value considering the specific application field, as described in the following three solutions.

First solution (T_{1-med}): The interference measured in the phantom layer depends on active UE positions. So, for each Ph-eNB $_i$, known the location of all active UEs, the users' median location ($P_{i,med}$) is derived by solving a 1-median problem [14]. The Euclidean distance, d_i , between $P_{i,med}$ and Ph-eNB $_i$ is calculated and inserted into vector D .

The threshold T is calculated once only, as follow:

$$T_{1-med} = \frac{1}{|D|} \cdot \sum_{i=1}^{|D|} d_i, \quad (2)$$

This threshold depends on users' distributions, so the clustering operation could be performed after a change in the active users' position and/or number. Consequently, the CRA version which adopts T_{1-med} (CRA_{1-med}) provides a dynamic clustering operation.

Second solution (T_{reg}): In a regular Ph-eNBs deployment (regular grid), the distance d between two neighbour Ph-eNBs is constant. The threshold T is established as $T_{reg} = d$. Let's note that T_{reg} just depends on Ph-eNBs locations and it does not change with traffic variation. Therefore, the MMDA output (K) and the final clusters topology returned by K-Means algorithm will not change once the Ph-eNBs network layout is fixed. So, the CRA version which adopts the threshold T_{reg} (CRA_{reg}) provides a static clustering operation. This means a lower computational complexity than the dynamic clustering operation.

Third solution (T_{rand}): For random Ph-eNBs deployment (random grid), with respect to regular grid case, the determination of threshold T is not straightforward. For each Ph-eNB $_i$, the Euclidean distance, d_{pi} , from the closest Ph-eNB is detected. These distances are inserted into vector D_p . Then, the threshold T is defined as follows:

$$T_{rand} = \frac{1}{|D_p|} \cdot \sum_{i=1}^{|D_p|} d_{pi}, \quad (3)$$

Also with this solution, T_{rand} value does not change with users' number and/or position. Therefore, known the Ph-eNB layout, the CRA version which adopts T_{rand} (CRA_{rand}), provides a unique cluster topology by a static clustering operation.

B. 2nd phase: Dynamic allocation of Cluster Resources

In the previous step the Ph-eNBs which have a critical interference relations were mapped onto the same cluster. Now, the centralized controller has to allocate clusters spectral resources based on users' demand. The whole spectral resource B must be subdivided and allocated in orthogonal way to the cell assigned with the same cluster taking into account the inter-cluster interference. For each cluster, we will try to:

- assign fairly resources to the cluster cells;
- use spectral resources in the most efficient way.

To fulfill these targets, the guidelines of our algorithm have been:

- make a polling operation between the cluster cells by allocating a spectral resource unit (a PRB, one channel in the following) at a time;
- choose the best candidate UE for each cell;
- minimize interference between clusters.

In a cluster, at every polling round, the candidate UEs for allocation of available PRBs are one per cell. It is the UE closest to its serving Ph-eNB, to achieve a better spectral efficiency.

For each candidate UE $_i$, the value of SINR (Υ_{ij}) is estimated on each channel j still available. The Ph-eNBs in other cluster which already use the channel j are consider as interfering. In order to maximize the spectral efficiency and the system capacity, the algorithm chooses the channel-user pair having the highest SINR. Polling operation terminates when all radio resources have been allocated, or when there is not further traffic demand by UEs. The details of our spectral resources allocation algorithm are described in the following pseudocode.

Algorithm 1: Dynamic Radio Resource Allocation

Definition

- * N_p^k : Ph-eNB number assigned to cluster C_k
 - * Cls_List : Cluster id list, sorted in descending order according to N_p^k value.
 - * ϕ_k : Unallocated channels into cluster C_k .
 - * $S_UE_{List}^i$: list of UEs attached to Ph-eNB $_i$ waiting to be served. They are sorted in ascending order according their distance to Ph-eNB $_i$.
 - * UE_{Firs}^i : First element of the $S_UE_{List}^i$. It is the candidate UE of the Ph-eNB $_i$.
 - * Γ_k : Is a $N_p^k \times |\phi_k|$ matrix, where the pair (i,j) contains Υ_{ij} of UE_{Firs}^i .
-

- 1: **for each** $C_k \in Cls_List$ **do**
 - 2: **repeat**
 - 3: **for each** $UE_{Firs}^i \in C_k$ and $j \in \phi_k$
 - 4: calculate the Υ_{ij} and insert it in Γ_k
 - 5: **end for**
 - 6: **repeat**
 - 7: find the pair (i,j) that maximises Υ_{ij} in Γ_k
 - 8: assign the channel j to UE_{Firs}^i and then delete i -th row and j -th column of Γ_k . Update $\phi_k = \phi_k \setminus j$
 - 9: **if** UE_{Firs}^i has an adequate number of channels which meet the required throughput **then**
 - 10: $S_UE_{List}^i = S_UE_{List}^i \setminus UE_{Firs}^i$ and update UE_{Firs}^i
 - 11: **end if**
 - 12: **until** Γ_k is empty
 - 13: **until** ϕ_k is empty or all UEs into C_k are served
 - 14: **end for**
-

IV. PERFORMANCE EVALUATION

The simulation scenario is composed of M Phantom cells distributed over a flat area of 200 m x 200 m to form a random or regular grid. The phantom cells area is partially overlapped.

We consider N active UEs uniformly distributed within the area considered. In the simulations, the maximum value of N is 120. It has been derived from the traffic model in [13] for a dense urban area characterized by 3000 citizen/km² on average. Each active UE requires 2Mbps.

To simulate signal attenuation between Ph-eNBs and UEs, we use the path loss model proposed in [3]. For an urban area and for a carrier frequency of 3.5 GHz, the path loss is:

$$PL[dB] = 35 + 39.4 \log_{10}(d_{m,n}), \quad (4)$$

where $d_{m,n}$ [m] is the distance between Ph-eNB $_m$ and the UE $_n$.

The set of parameters used in simulations is provided in Table I. The performance is assessed by MATLAB environment and the simulation results are averaged over 50 independent simulations.

Let's note that the CTRM algorithm has been proposed for indoor femtocells with low transmission power (maximum radius 10m) and only one user. So, the spectral allocation is applied at Femto eNB level. Instead, in the considered outdoor environment where the Ph-eNBs have a maximum radius of 100 m and more connected UEs, our resource allocation is done at UE level to achieve a major efficiency. To fairly assess control schemes, the benchmark in [10] is adapted to the outdoor phantom cell scenario. So, the two-stage sub-channel allocation scheme is substituted with our spectral resource allocation algorithm. In this way, the fundamental difference between these control schemes is in the clustering procedure. More specifically, in the determination of T, CTRM uses the traditional MMDA by using (1).

As regards the Graph scheme proposed in [11], it can be applied unchanged because it is based on scenarios which have similar features with those considered in this paper.

As performance metrics, we consider the total throughput of phantom cell layer and the throughput improvement compared to no-partition scheme. On basis of measured SINR, a UE requires a different number of PRBs for equals service bit rate. Therefore, if there is not an appropriate RRM control then the resources may not be enough to fulfill the traffic demands causing a disservice. So, we define the "Disservice" as percentage of disregarded traffic demand:

$$Disservice = \frac{Total\ Required\ Load\ [Mbps] - Total\ Thr\ [Mbps]}{Total\ Required\ Load\ [Mbps]} \quad (5)$$

TABLE I. SYSTEM PARAMETERS

Parameter	Symbol	Value
System bandwidth	B	10 MHz
Total number of available PRBs per B	$PRBs_T$	50
Carrier frequency	f_c	3.5 GHz
Channel bandwidth per PRB	ΔB	180 KHz
Number of Ph-eNBs	M	[4, ..., 49]
Number of active UEs	N	[20, ..., 120]
Maximum Ph-eNB TX power	$P_{TX,max}$	24 dBm
Minimal required value for DRSRP	$DRSRP_{min}$	-124 dBm
Ph-eNB TX power per channel (j)	$P_{TX,i}$	7 dBm
Noise power per channel	N	-114.5 dBm
Modulation schemes		QPSK, 16-QAM, 64-QAM

Case Regular Grid.

With only 4 Ph-eNBs, Fig. 2 shows the percentage of throughput improvement compared with the no-partition scheme, under different traffic intensity (active UE number). We can see that our control scheme CRA_1-med exhibits the best performance like ones achieved by the CTRM. However, the scenario with only 4 Ph-eNBs is not ultra-dense. Contrary, in the ultra-dense case with 49 Ph-eNBs, Fig. 3 shows that the CRTM performance degrades compared with our CRA (in both static and dynamic variants). This comparison confirms that the CTRM has been thought for an indoor scheme where a relatively low interference is experimented. Therefore, in outdoor environment of small cells (maximum radius about

100 m), the CTRM can achieve good performance only if the interference is reduced. This is possible decreasing density of cells and/or traffic intensity.

Case Random Grid.

For an ultra-dense scenario with 49 cells in random deployments, in figures 4a and 4b, we note that when traffic density increases the performances of the CRA_rand and CRA_1-med outperform both CTRM and Graph scheme, in terms of throughput improvement and disservice. The reason is that in the clustering procedure the CTRM scheme does not take account of critical interference relations among the Ph-eNBs (obtaining low K values), while the Graph scheme allocates the radio resources regardless of traffic intensity within each Ph-eNB.

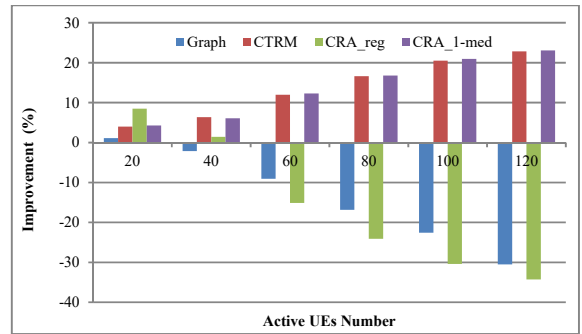


Fig. 2. Throughput improvement in a regular deployment with 4 Ph-eNBs.

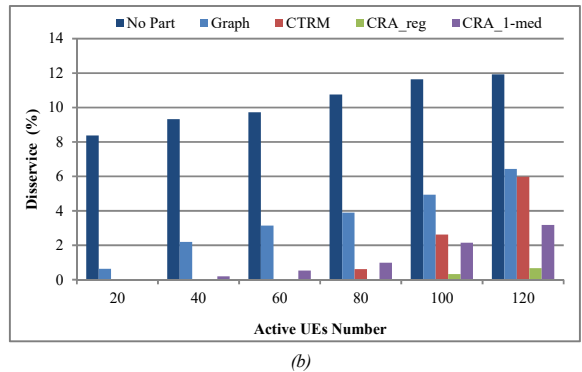
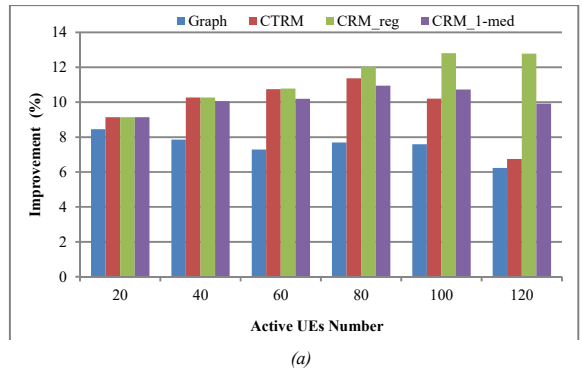
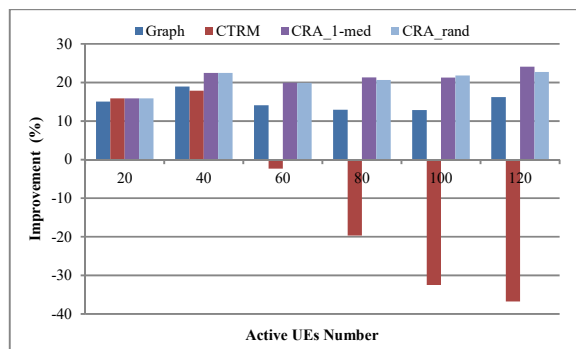
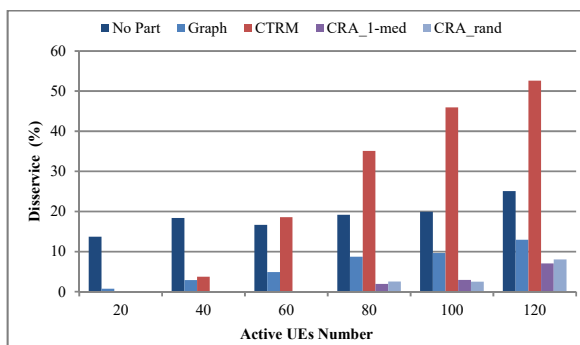


Fig. 3. Regular deployment with 49 Ph-eNBs. (a) Improvement in throughput and (b) Disservice vs number of traffic intensity.



(a)



(b)

Fig. 4. Random deployment with 49 Ph-eNBs. (a) Improvement in throughput and (b) Disservice vs number of traffic intensity.

Finally, in high-traffic condition (120 connected UEs in the considered area), the total throughput as a function of the Ph-eNB density is plotted in Fig. 5. These results confirm that CRA_rand is the best choice, in fact it works well with any cell density (with 400 cell/Km² and beyond), without requiring the same computational complexity of dynamic clustering procedure. Unlike the CRA_1-med, CRA_rand has not to address the hard issue of identifying how often the clustering procedure (periodic or event-triggered) should be done.

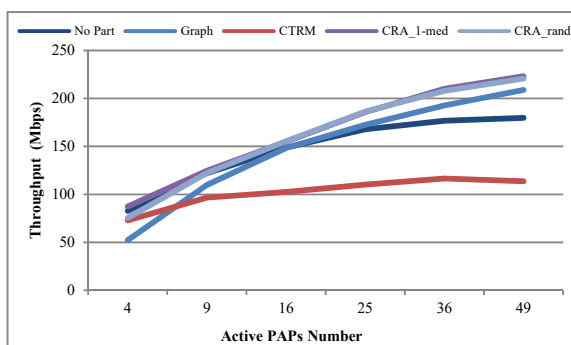


Fig. 5. Total throughput vs number of Phantom cells

V. CONCLUSION

In this paper, we propose a new radio resource manager control, CRA, that allows to allocate the spectral resources in an ultra-dense phantom network. CRA scheme is based on cell clustering concept. This scheme is suitable for outdoor environments with several hotspots which have moderate-power base stations and a large number of connected UEs into their own coverage area.

Our control scheme is composed of two phases. In the first phase, the Ph-eNBs are grouped in communities (clusters) by using modified Max-Min distance algorithm and k-means algorithm. Whereas in the second phase, the spectral resource allocation algorithm is run to allocate cluster bandwidth resources to the cells based on actual users' demand of traffic.

We propose three variants of CRA: CRA_1-med executes a dynamic clustering operation based on the users' position; CRA_reg and CRA_rand execute static clustering operation based on Ph-eNBs deployment (regular or random grid). The performance evaluation we did in different network deployments allowed us to prove that the CRA_rand solution achieves similar performance to the CRA_1-med with less computational complexity. Unlike the CRA_1-med, CRA_rand has not to address the hard issue of identifying how often the clustering procedure (periodic or event-triggered) should be done. In addition, the system level simulations show that our control scheme CRA_rand outperforms two reference schemes (CTRM and Graph) in terms of throughput and QoS.

REFERENCES

- [1] Cisco Visual Networking Index, "Global Mobile Data Traffic Forecast Update, 2011-2016", White Paper, Feb. 2012.
- [2] 3GPP Technical specification group radio access network; Study on Small Cell enhancement for E-UTRA and E-UTRAN; Higher layer aspects (Rel.12) [3GPP TR 36.842 v12.0.0], Dec. 2013.
- [3] H.Ishii, Y.Kishiyama, H.Takahashi, "A novel architecture for LTE-B: C-plane/U-plane split and Phantom Cell concept", in Globecom Workshops, 2012 IEEE, Anaheim, CA, pp. 624-630.
- [4] Tenon et al, "Performance evaluation of macro-assisted small cell energy savings scheme", in EURASIP Journal on Wireless Communications and Networking, 2015, doi:10.1186/s13638-015-0432-0,
- [5] 3GPP, Technical specification group radio access network; 3GPP TSG RAN WG1 R1-140213, Discovery Signal Design for Small Cell On/Off.
- [6] M.Ding, et al. "Will the area spectral efficiency monotonically grow as small cells go dense?" in Proc. IEEE Glob. Commun. Conf (GLOBECOM), San Diego, CA, USA, Dec. 2015, pp. 1-7.
- [7] J. Leskovec, A. Rajaraman, J.D. Ullman, "Mining of massive datasets", <http://infolab.stanford.edu/~ullman/mmds/book.pdf>
- [8] L.Cheng, et al., "A Cooperative Resource Allocation Scheme Based on SON in Ultra-Dense Small Cell Deployment.", 81st Vehicular Technology Confer (Spring), 2015 IEEE, Glasgow, Schottland, pp. 1-6.
- [9] L. Bai, T. Liu, Z. Chen, C. Yang, "A graph-based interference topology control for ultra-dense network.", in 12th Intern. Conf. on Signal Processing (ICSP), HangZhou, China, pp. 1676-1681, Oct. 2014.
- [10] R. Wei, Y. Wang, Y.Zhang, "A Two-Stage Cluster-Based Resource Management Scheme in Ultra-Dense Networks.", in Intern. Conf. on Comm. (ICCC), 2014 IEEE/ICCC, Shanghai China, pp. 738-742.
- [11] A. Dudnikova, P. Dini, L. Giupponi, D. Panno, "Multi-criteria decision for small cell switch off in ultra-dense LTE networks." in 13th Intern. Confer. on Telecomm.(ConTEL), Graz, Austria, pp. 1-8, Jul. 2015.

- [12] L. Liu, V. Garcia, L. Tian, Z. Pan, J. Shi, "Joint cluster and inter-cell resource allocation for CoMP in ultra dense cellular network.", in *Intern. Conf. on Comm. (ICC), 2015 IEEE, London*, pp. 2560-2564.
- [13] ICT-EARTH, D2.3, "Energy Efficiency Analysis of the Reference Systems, Areas of Improvements and Target Breakdown", *EARTH Project Deliver. Tech. Rep. Dec 2010*.
- [14] S. Gallo, "Antipole clustering",
http://sangi1981.altervista.org/20_antipoleClustering.html
- [15] A. Mastro Simone, D. Panno, "A comparative analysis of mmWave vs LTE technology for 5G Moving Network.", *11th Int. Conf. on Wireless and Mobile Comp., Netw. and Comm. (WiMob), 2015 IEEE, Abu Dhabi*, pp. 422-429.
- [16] CEE 6150, *Digital Image Processing, "Unsupervised Classification"*,
<http://ceeserver.cee.cornell.edu>
- [17] Akyildiz Ian F, Wang Pu, Lin Shih-Chun. 2015. *SoftAir: a software defined networking architecture for 5G wireless systems. Computer Networks*, vol 85, 5 July 2015:pp 1-18